第38卷第1期 2022年1月
无 机 化 学 学 报 CHINESE JOURNAL OF INORGANIC CHEMISTRY
Vol.38 No.1 145-152

多齿席夫碱配体构筑的$Ln^{Ⅲ}_2$配合物的晶体结构及磁性

高晓丽[1] 雷文婷[1] 张清芳[1] 周 宇[1] 康晓敏*[,2]
([1]太原师范学院化学系,晋中 030619)
([2]内蒙古大学化学化工学院,呼和浩特 010021)

摘要: 使用多齿席夫碱配体,通过溶剂热法,设计与合成了3例新的稀土配合物$[Ln_2(L)_2(acac)_2(CH_3OH)_2]\cdot 2CH_3OH$(Ln=Sm (**1**)、Gd (**2**)、Ho (**3**),H_2L=吡啶-2-羧酸-(1-甲基-3-氧代丁烯基)-酰肼),并对配合物**1**~**3**的结构与磁性质进行了系统的研究。单晶结构测试结果表明配合物**1**~**3**为同构,每个中心稀土Ln(Ⅲ)离子为八配位,其配位几何构型为扭曲的四方反棱柱;相邻的中心稀土Ln(Ⅲ)离子通过2个μ_2-O连接形成了平行四边形的$[Ln_2O_2]$核心。磁性测试揭示配合物**2**具有磁制冷性质,其最大磁熵变($-\Delta S_{max}$)为31.9 $J\cdot K^{-1}\cdot kg^{-1}$($T$=2.0 K,$\Delta H$=70 kOe);配合物**3**表现出了慢磁驰豫行为。

关键词: $Ln^{Ⅲ}_2$配合物; 晶体结构; 磁性; 磁制冷性质; 慢磁驰豫行为
中图分类号: O614.33+7; O614.33+9; O614.343 **文献标识码:** A **文章编号:** 1001-4861(2022)01-0145-08
DOI: 10.11862/CJIC.2022.002

Crystal Structures and Magnetic Properties of $Ln^{Ⅲ}_2$ Complexes Based on a Polydentate Schiff Base Ligand

GAO Xiao-Li[1] LEI Wen-Ting[1] ZHANG Qing-Fang[1] ZHOU Yu[1] KANG Xiao-Min*[,2]
([1]*Department of Chemistry, Taiyuan Normal University, Jinzhong, Shanxi* 030619, *China*)
([2]*College of Chemistry and Chemical Engineering, Inner Mongolia University, Hohhot* 010021, *China*)

Abstract: Three new $Ln^{Ⅲ}_2$ complexes based on a polydentate Schiff base ligand, namely $[Ln_2(L)_2(acac)_2(CH_3OH)_2]\cdot 2CH_3OH$ (Ln=Sm (**1**), Gd (**2**), Ho (**3**), H_2L=pyridine-2-carboxylic acid (1-methyl-3-oxo-butylidene)-hydrazide, Hacac =acetylacetone), have been synthesized by using solvothermal method. The crystal structures and magnetic properties of these complexes have been systematically studied. The crystal structures measurement results reveal that complexes **1**-**3** are isostructural and each eight-coordinated Ln(Ⅲ) ion possesses a square antiprism geometry; the adjacent central rare earth Ln(Ⅲ) ions are connected by two μ_2-O to form a parallelogram $[Ln_2O_2]$ core. The magnetic study showed that complex **2** displayed significant magnetic refrigeration property with a larger magnetic entropy ($-\Delta S_{max}$) of 31.9 $J\cdot K^{-1}\cdot kg^{-1}$ at ΔH=70 kOe and T=2.0 K; while complex **3** shows slow magnetic relaxation behavior. CCDC: 2052182, **1**; 2052183, **2**; 2052184, **3**.

Keywords: $Ln^{Ⅲ}_2$ complexes; crystal structures; magnetic properties; magnetic refrigeration property; slow magnetic relaxation behavior

0 Introduction

In recent years, the study of lanthanide-based complexes has attracted increasing attention of chemists and material scientists not only due to their beautiful and fascinating crystal structures but also because of the potential applications in functional materials, including interesting magnetic properties, lumines-

收稿日期:2021-06-04。收修改稿日期:2021-10-23。
国家自然科学基金(No.21671124)资助。
*通信联系人。E-mail:kangxm2020@163.com

cence, gas adsorption, and catalysis[1-4]. Among these potential applications of lanthanide-based complexes, the molecular-based magnetic material is one of the research hotspots for inorganic chemistry and material chemists[5], and magnetic refrigeration and single-molecule magnets (SMMs) are particularly attractive[6-9]. Key to the potential magnetic refrigeration application of molecular-based magnetic materials is its large magnetocaloric effect (MCE)[10], and an excellent magnetic refrigeration material featuring large MCE should possess negligible magnetic anisotropy and a large magnetic density[11]. Hence, the isotropic Gd(Ⅲ) ion with a high spin state (S=7/2) is the best candidate for designing and constructing Ln(Ⅲ)-based complexes, which would be a promising magnetic refrigerant material to perform significant MCE[12]. Based on this, lots of polynuclear or high-nuclear Gd(Ⅲ)-based clusters with fascinating structures and larger MCE have been reported over the past decade[13-16]. It is worth mentioning that Zheng and Long′s group has conducted outstanding work on the magnetic refrigeration materials of Gd(Ⅲ)-based clusters[17-18]. These studies promote the design and synthesis of lanthanide-based complexes with outstanding and excellent magnetic properties. On the other hand, lanthanide-based SMMs have caused public attention in recent years[19], and designing lanthanide-based SMMs with large energy barriers (U_{eff}) and high blocking temperatures (T_B) is a great challenge[20]. Given this, lots of Ln(Ⅲ)-based SMMs exhibiting significant magnetic behavior have appeared since the first Ln(Ⅲ)-based SMM $(Bu_4N)[Tb(Pc)_2]$ reported by Ishikawa et al. in 2003[21].

To seek and study the magnetic behaviors of lanthanide-based complexes, an attractive polydentate ligand H_2L (Scheme 1) has been selected to construct lanthanide complexes, and three $Ln^{Ⅲ}_2$ complexes $[Ln_2(L)_2(acac)_2(CH_3OH)_2]\cdot 2CH_3OH$ (Ln(Ⅲ)=Sm (**1**), Gd (**2**), and Ho (**3**), H_2L=pyridine-2-carboxylic acid (1-methyl-3-oxo-butylidene)-hydrazide, Hacac=acetylacetone) have been synthesized. The magnetic refrigeration and slow magnetic relaxation behavior of **1**-**3** have been studied.

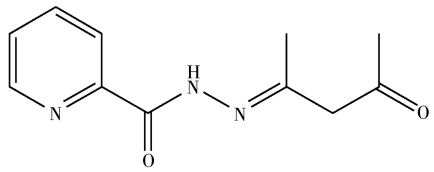

Scheme 1 Structure of ligand H_2L

1 Experimental

1.1 Material and measurement

Solvents (methanol, dichloromethane) and starting chemical reagent ($Ln(NO_3)_3\cdot 6H_2O$, Ln=Sm, Gd, and Ho) were purchased commercially and used without further purification. Acetylacetone and 2-pyridine carboxylic acid hydrazide were purchased from Aladdin Reagent (Shanghai) Co., Ltd. $Ln(acac)_3\cdot 2H_2O$ (Ln=Sm, Gd, and Ho) was prepared using a reported method[22]. The elemental analyses (C, H, and N) of complexes **1**-**3** were measured on a PerkinElmer 240 CHN elemental analyzer. Powder X-ray diffraction (PXRD) of complexes **1**-**3** were performed using an Ultima Ⅳ (Rigaku) with Cu $K\alpha$ radiation in a 2θ range from 5° to 50°. The operating voltage and current were 40 kV and 25 mA, respectively. Thermogravimetric analyses (TGA) of complexes **1**-**3** were performed on a TG 209 apparatus (Netzsch) under an air atmosphere. Magnetic properties for complexes **1**-**3** were measured using a Quantum Design MPMS-XL7 and a PPMS-9 ACMS magnetometer. Diamagnetic corrections were estimated with Pascal′s constants for all atoms[23].

1.2 Preparation of complexes 1-3

2-Pyridine carboxylic acid hydrazide (0.04 mmol), $Ln(acac)_3\cdot 2H_2O$ (0.04 mmol, Ln=Sm (**1**), Gd (**2**), and Ho (**3**)), methanol (8 mL), and dichloromethane (2.0 mL) were enclosed in a 15 mL glass vial, and then the mixture was stirred at room temperature for about 2.0 h. Whereafter, the mixture was heated to 70 ℃ and kept for 48 h, and then the temperature was decreased to room temperature slowly. Yellow block crystals suitable for X-ray diffraction were obtained.

$[Sm_2(L)_2(acac)_2(CH_3OH)_2]\cdot 2CH_3OH$ (**1**): Yield based on $Sm(acac)_3\cdot 2H_2O$: 36%. Elemental analysis Calcd. for $C_{36}H_{52}N_6O_{12}Sm_2$(%): C 40.66, H 4.89, N 7.91; Found (%): C 40.64, H 5.03, N 8.00.

$[Gd_2(L)_2(acac)_2(CH_3OH)_2]\cdot 2CH_3OH$ (**2**): Yield based

on $Gd(acac)_3\cdot 2H_2O$: 32%. Elemental analysis Calcd. for $C_{36}H_{52}N_6O_{12}Gd_2$(%): C 40.10, H 5.01, N 7.80; Found (%): C 40.21, H 4.97, N 7.75.

$[Ho_2(L)_2(acac)_2(CH_3OH)_2]\cdot 2CH_3OH$ (**3**): Yield based on $Ho(acac)_3\cdot 2H_2O$: 41%. Elemental analysis Calcd. for $C_{36}H_{52}N_6O_{12}Ho_2$(%): C 39.57, H 4.76, N 7.69; Found (%): C 39.62, H 4.89, N 7.72.

1.3 X-ray crystallography

The X-ray diffraction measurements for complexes **1**-**3** were performed on a Bruker SMART APEX Ⅱ CCD diffractometer equipped with a graphite monochromatized Mo $K\alpha$ radiation (λ =0.071 073 nm) by using φ-ω scan mode. Multi-scan absorption correction was applied to the intensity data using the SADABS program. The structures were solved by direct methods and refined by full-matrix least-squares on F^2 using the SHELXTL-2018 program. All non-hydrogen atoms were refined anisotropically. All the other H atoms were positioned geometrically and refined using a riding model. Details of the crystal data and structure refinement parameters for **1**-**3** are summarized in Table 1, and selected bond lengths and angles of **1**-**3** are listed in Table S1-S3 (Supporting information).

CCDC: 2052182, **1**; 2052183, **2**; 2052184, **3**.

Table 1　Crystal data and structure refinement parameters for complexes 1-3

Parameter	1	2	3
Empirical formula	$C_{36}H_{52}N_6O_{12}Sm_2$	$C_{36}H_{52}N_6O_{12}Gd_2$	$C_{36}H_{52}N_6O_{12}Ho_2$
Formula weight	1 062.46	1 075.25	1 091.62
T / K	150(2)	293(2)	153(2)
Crystal system	Monoclinic	Monoclinic	Monoclinic
Space group	$P2_1/c$	$P2_1/c$	$P2_1/c$
a / nm	0.773 0(5)	0.777 6(6)	0.765 59(3)
b / nm	2.118 3(3)	2.131 2(6)	2.117 2(3)
c / nm	2.579 3(7)	2.594 7(1)	2.574 5(7)
β / (°)	93.961(2)	92.993 0(15)	93.437 5(15)
V / nm^3	4.213 8(5)	4.294 6(2)	4.165 7(3)
Z	4	4	4
Cryst size / mm	0.25 × 0.21 × 0.14	0.25 × 0.17 × 0.11	0.27 × 0.21 × 0.14
D_c / ($g\cdot cm^{-3}$)	1.574	1.582	1.639
μ / mm^{-1}	2.816	18.867	3.828
Limiting indices	$-9 \leqslant h \leqslant 9$,	$-8 \leqslant h \leqslant 9$,	$-9 \leqslant h \leqslant 9$,
	$-26 \leqslant k \leqslant 26$,	$-18 \leqslant k \leqslant 26$,	$-26 \leqslant k \leqslant 26$,
	$-32 \leqslant l \leqslant 31$	$-27 \leqslant l \leqslant 32$	$-32 \leqslant l \leqslant 32$
Reflection collected	67 691	17 142	52 003
Unique	8 647	8 364	8 552
Parameter	485	485	485
R_{int}	0.091 5	0.042 2	0.066 8
GOF on F^2	1.006	1.084	1.085
R_1, wR_2 [$I>2\sigma(I)$]	0.045 2, 0.100 2	0.068 6, 0.182 5	0.042 7, 0.095 1
R_1, wR_2 (all data)	0.073 6, 0.113 7	0.071 3, 0.184 5	0.060 2, 0.101 7

2 Results and discussion

2.1 Crystal structures of complexes 1-3

Single-crystal X-ray diffraction analyses reveal that **1**-**3** are isostructural and crystallize in the monoclinic space group $P2_1/c$ (Table 1). Hereon, we selected the structure of **2** as a representative for describing. As shown in Fig.1, the structure of **2** comprises two Gd(Ⅲ) ions, two L^{2-}, two $acac^-$, and two coordinated CH_3OH. Each central Gd(Ⅲ) ion is coordinated by six oxygen atoms and two nitrogen atoms formed a $[N_2O_6]$ coordination environment. As shown in Fig.S1, the Gd1 ion is

coordinated by two nitrogen atoms (N3 and N4) and six oxygen atoms (O2, O3, O4, O7, O8, and O9) of two L^{2-}, one CH_3OH and one $acac^-$. The eight-coordinated Gd1 ion possesses a square antiprism geometry which is confirmed by using SHAPE 2.0 software (Table 2). The coordination mode of L^{2-} and $acac^-$ are shown in Fig.2. The two central Gd(Ⅲ) ions are connected by two μ_2-O atoms forming a parallelogram $[Gd_2O_2]$ core. In the $[Gd_2O_2]$ core, the Gd1…Gd2 distance is 0.392 8(8) nm, O2—Gd1—O4 bond angle is 62.201 1(9)°, and the Gd1—O2—Gd2 bond angle is 113.809 2(3)°. Furthermore, the bond distances of Gd—O in complex **2** are in a range of 0.225 0(6)-0.244 5(6) nm, and the Gd1—N3, Gd1—N4, Gd2—N1, and Gd2—N6 bond lengths are 0.255 5(8), 0.243 8(7), 0.242 6(7), and 0.254 1(8) nm, respectively. The O—Gd—O bond angles are in a range of 66.18(19)°-147.9(2)°. These bond lengths and angles of **2** are compared to those of reported Gd_2 complexes[24-27].

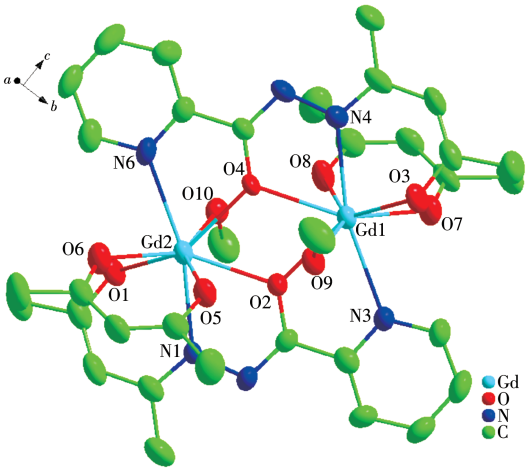

H atoms are omitted for clarity

Fig.1 Molecular structure of complex **2** shown with 30% probability displacement ellipsoids

Table 2 Gd(Ⅲ) geometry analysis by SHAPE 2.0 for complex 2

Gd(Ⅲ) ion	D_{4d} SAPR	D_{2d} TDD	C_{2v} JBTPR	C_{2v} BTPR	D_{2d} JSD
Gd1	2.193	2.379	3.673	2.582	5.883
Gd2	2.185	2.211	3.656	2.511	5.749

SAPR-8=square antiprism; TDD-8=triangular dodecahedron; JBTPR-8=biaugmented trigonal prism J50; BTPR-8=biaugmented trigonal prism; JSD-8=snub diphenoid J84; The number 8 represents eight-coordinated geometrical configuration.

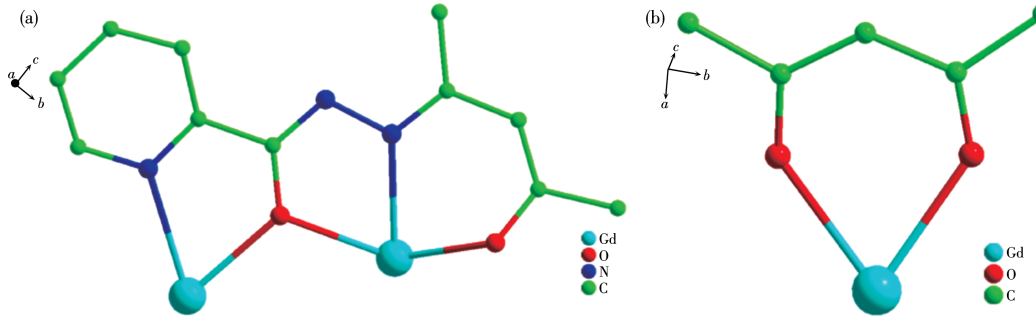

H atoms of C—H bonds are omitted for clarity

Fig.2 (a) Coordination mode of L^{2-} in **2**; (b) Coordination mode of $acac^-$ in **2**

2.2 PXRD pattern and TGA

To prove the phase purities of complexes **1-3**, the crystalline products of these complexes were measured by PXRD. As shown in Fig.S2, the PXRD patterns of the crystalline samples of **1-3** were in good agreement with their simulated ones, which proves the high phase purity.

To investigate the thermal stabilities of complexes **1-3**, TGA was performed under an air atmosphere. As shown in Fig.S3, the TG curves of **1-3** showed a similar variation trend. Hereon, we selected the TG curve of complex **1** for a detailed description. The weight loss of 6.31% (Calcd. 6.02%) between 40 and 294 ℃ can be attributed to the loss of two free CH_3OH. After that, complex **1** decomposed gradually.

2.3 Magnetic properties

The magnetic susceptibility data for the $Ln^{Ⅲ}_2$ complexes (**1-3**) were measured with the polycrystalline

samples during a temperature range of 2.0 to 300.0 K and under an external magnetic field of 1.0 kOe. The $\chi_M T$ vs T plots for complexes **1-3** are shown in Fig.3. At 300.0 K, the $\chi_M T$ values of **1-3** were 2.40, 15.73, and 28.20 $cm^3 \cdot mol^{-1} \cdot K$, respectively. The expected values for two free Ln(Ⅲ) ions are shown as follows: two isolated Sm(Ⅲ) ions ($^6H_{5/2}$, g=2/7) gave 0.95 $cm^3 \cdot mol^{-1} \cdot K$ for **1**; two isolated Gd(Ⅲ) ions ($^8S_{7/2}$, g=2) gave 15.76 $cm^3 \cdot mol^{-1} \cdot K$ for **2**; two isolated Ho(Ⅲ) ions ($^5I_8$, g=4/5) gave 28.14 $cm^3 \cdot mol^{-1} \cdot K$ for **3**. For **1**, as the temperature decreased, the $\chi_M T$ value slowly declined and reached the minor value of 0.26 $cm^3 \cdot mol^{-1} \cdot K$ at 2.0 K. For **2**, during the temperature range of 20.0-300.0 K, the $\chi_M T$ value almos remained constant; whereafter, the $\chi_M T$ value dropped to a minimum of 10.83 $cm^3 \cdot mol^{-1} \cdot K$ at 2.0 K. The downtrend suggests that there is an antiferromagnetic interaction between adjacent Gd(Ⅲ) ions in complex **2**[28]. For **3**, the $\chi_M T$ value decreased slowly from 300 to 50 K, then it decreased quickly to reach the minimum of 7.01 $cm^3 \cdot mol^{-1} \cdot K$ at 2.0 K. This behavior may be attributed to the thermal depopulation of the Ho(Ⅲ) Stark sublevels or/and the antiferromagnetic interactions between the adjacent Ho (Ⅲ) ions in complex **3**[29].

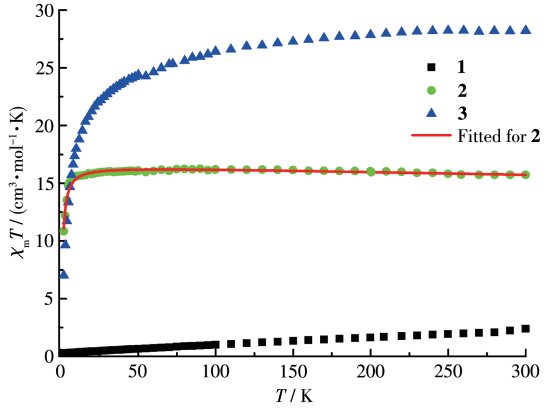

Red solid line stands for the best fitting of complex **2** by using Eq.**1**

Fig.3　Temperature dependence of $\chi_M T$ at 1.0 kOe for **1-3**

The Curie - Weiss law was used for fitting the magnetic susceptibility of **2** (Fig.S4). Two parameters C (15.83 $cm^3 \cdot mol^{-1} \cdot K$) and θ (−0.73 K) were obtained (R =0.999 78). The small and negative θ value of **2** further suggests that there is an antiferromagnetic interaction between adjacent Gd(Ⅲ) ions in **2**[30]. For further exploring the magnetic interaction between the adjacent Gd(Ⅲ) ions in complex **2**, we fitted the $\chi_M T$ vs T curve of **2** by using the Hamiltonian: $\hat{H}_{Gd_2} = -J(\hat{S}_{Gd_1}\hat{S}_{Gd_2}) - g\mu_B\hat{H}(\hat{S}_{Gd_1} + \hat{S}_{Gd_2})$ (**1**)[31], and the two significant parameters, J=−0.06 cm^{-1} and g=2.05, were obtained. The negative J value further proves that there is an antiferromagnetic coupling between the neighboring Gd (Ⅲ) ions in **2**.

The magnetization data for complex **2** were studied at 2.0-10.0 K in a 0-70 kOe field. As depicted in Fig. 4, the magnetization M for complex **2** rapidly increased blow 20 kOe and then steadily increased to 14.02$N\beta$ at 70 kOe, which is very close to the saturation value of 14$N\beta$ for two free Gd(Ⅲ) (S=7/2, g=2) ions.

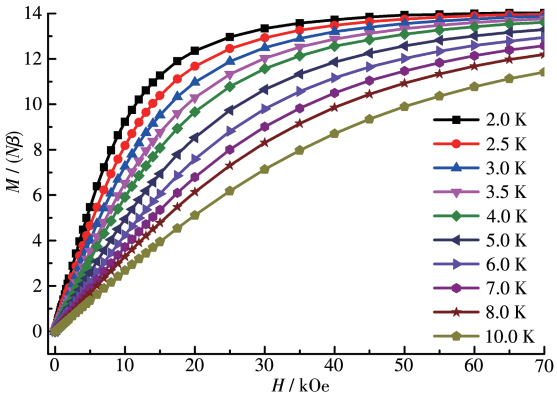

Fig.4　Plots of M vs H at 2.0-10.0 K for **2**

According to the previous literature[32-34], due to the presence of the isotropic Gd(Ⅲ) ion with a high-spin ground state, hereon, the magnetocaloric effect of complex **2** was investigated. The maximum magnetic entropy change ($-\Delta S_{max}$) could be calculated by using the Maxwell equation: $\Delta S_{max}(T) = \int[\partial M(T,H)/\partial T]_H dH$[35]. As shown in Fig. 5, at ΔH=70 kOe and T=2.0 K, the observed $-\Delta S_{max}$ was 31.9 $J \cdot K^{-1} \cdot kg^{-1}$, which was smaller than the theoretical value of 34.2 $J \cdot K^{-1} \cdot kg^{-1}$ based on the equation: ΔS_{max}=$2R\ln(2S+1)$ (S_{Gd}=7/2 and R= 8.314 $J \cdot mol^{-1} \cdot K^{-1}$). The difference between experimental and theoretical magnetic entropy change ($-\Delta S_{max}$) may be due to the weak antiferromagnetic interactions between Gd(Ⅲ) ions in complex **2**[36]. It is worth mentioning that the $-\Delta S_{max}$ of complex **2** was larger than those

of mostly reported Gd_2 complexes[37-39]. With the larger $-\Delta S_{max}$ value, complex **2** may be a good candidate for potential application in magnetocaloric materials.

In order to study the dynamic magnetic behavior of complex **3**, the alternating current (ac) magnetic susceptibility measurements were performed during a temperature range of 2.0-15.0 K at various frequencies. Clear frequency dependence of out-of-phase (χ'') signals was observed which suggests that slow magnetic relaxation occurred in **3**[40]. However, no χ'' peaks were observed until T=2.0 K, and χ'' values gradually increased in the lower temperature region, which can be ascribed to the quantum tunneling effect (QTE)[41]. This phenomenon commonly occurred in most Ln(Ⅲ)-based complexes[42].

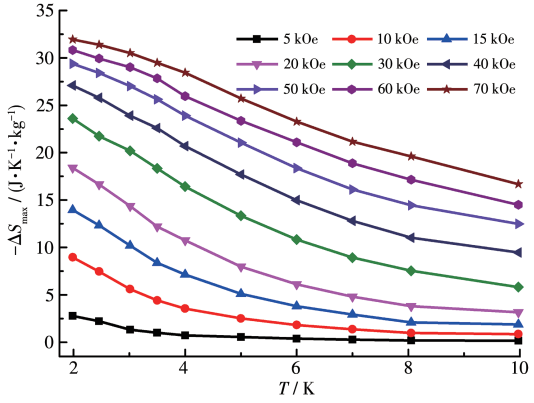

Fig.5 Plots of $-\Delta S_{max}$ vs T for **2**

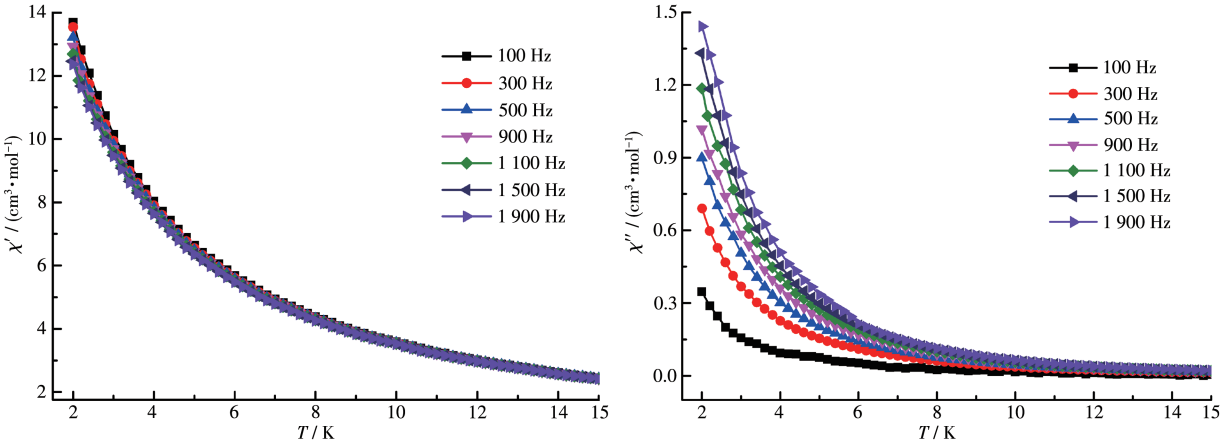

Fig.6 Temperature dependence of in-phase (χ') and out-of-phase (χ'') components of ac magnetic susceptibility for **3** in 0 Oe field with an oscillation of 3.0 Oe

To check the quantum tunneling of magnetization (QTM) effect above 2.0 K in complex **3**, under H_{dc}=2 500 Oe, the variable-temperature ac susceptibilities were determined. As shown in Fig.S5, remarkable and peak shapes were observed, which show that the QTE in complex **3** was pronounced, and the QTM effect was basically suppressed when it was under an external 2 500 Oe dc field. The ln τ vs T^{-1} plot is shown in Fig.7. The relaxation time τ obeys the Arrhenius law: $\tau=\tau_0\exp[\Delta E/(k_BT)]$. Two key parameters, energy barrier $\Delta E/k_B$=17.99 K and pre-exponential factor τ_0=9.55×10^{-7} s, were obtained. The τ_0 of complex **3** was consistent with the reported values of 10^{-6}-10^{-12} s for Ln(Ⅲ)-based SMMs[43-44].

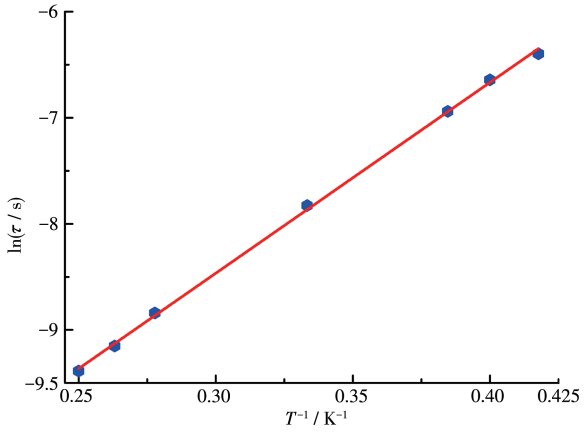

Red solid lines represent the best fit of the experimental data to the Arrhenius law

Fig.7 ln τ vs T^{-1} plot for complex **3**

3 Conclusions

In summary, we have synthesized three new $Ln^{Ⅲ}_2$ complexes $[Ln_2(L)_2(acac)_2(CH_3OH)_2]\cdot 2CH_3OH$ (Ln=Sm

(**1**), Gd (**2**), Ho (**3**)). Complexes **1**-**3** are all isostructural and contain a parallelogram [Ln_2O_2] core. Magnetic measurements imply that Gd_2 complex **2** displayed significant magnetic refrigeration property with a larger $-\Delta S_{max}$ of 31.9 $J\cdot K^{-1}\cdot kg^{-1}$ (ΔH=70 kOe and T=2.0 K); while Ho_2 complex **3** shows slow magnetic relaxation behavior.

Supporting information is available at http://www.wjhxxb.cn

References:

[1]Liu J L, Chen Y C, Tong M L. Symmetry Strategies for High Performance Lanthanide-Based Single-Molecule Magnets. *Chem. Soc. Rev.*, **2018**,**47**:2431-2453

[2]郑欢, 焦媛, 冯思思. 基于3,4′,5-联苯三羧酸构筑的钕配合物的合成、结构、荧光、光催化及磁性质. 无机化学学报, **2021**,**37**(9):1691-1699
ZHENG H, JIAO Y, FENG S S. Synthesis, Structure, Luminescence, Photocatalytic and Magnetic Properties of a Neodymium Complex Constructed from Biphenyl-3,4′,5-tricarboxylic Acid. *Chinese J. Inorg. Chem.*, **2021**,**37**(9):1691-1699

[3]Mahata P, Mondal S K, Singha D K, Majee P. Luminescent Rare-Earth-Based MOFs as Optical Sensors. *Dalton Trans.*, **2017**,**46**:301-328

[4]Li Y Z, Wang H H, Wang G D, Hou L, Wang Y Y, Zhu Z H. A Dy_6-Cluster-Based *fcu*-MOF with Efficient Separation of C_2H_2/C_2H_4 and Selective Adsorption of Benzene. *Inorg. Chem. Front.*, **2021**, **8**: 376-382

[5]Zhou N, Ma Y, Wang C, Xu G F, Tang J K, Xu J X, Yan S P, Cheng P, Li L C, Liao D Z. A Monometallic Tri-spin Single-Molecule Magnet Based on Rare Earth Radicals. *Dalton Trans.*, **2009**,**38**:8489-8492

[6]Bar A K, Kalita P, Singh M K, Rajaraman G, Chandrasekhar V. Low-Coordinate Mononuclear Lanthanide Complexes as Molecular Nanomagnets. *Coord. Chem. Rev.*, **2018**,**367**:163-216

[7]Guo Y N, Xu G F, Guo Y, Tang J K. Relaxation Dynamics of Dysprosium(Ⅲ) Single Molecule Magnets. *Dalton Trans.*, **2011**,**40**:9953-9963

[8]Zheng Y Z, Zhou G J, Zheng Z P, Winpenny R E P. Molecule-Based Magnetic Coolers. *Chem. Soc. Rev.*, **2014**,**43**:1462-1475

[9]Dong J, Cui P, Shi P F, Cheng P, Zhao B. Ultrastrong Alkali-Resisting Lanthanide-Zeolites Assembled by [Ln_{60}] Nanocages. *J. Am. Chem., Soc.*, **2015**,**137**:15988-15991

[10]Chen Y C, Prokleška J, Xu W J, Liu J L, Liu J, Zhang W X, Jia J H, Sechovský V, Tong M L. A Brilliant Cryogenic Magnetic Coolant: Magnetic and Magnetocaloric Study of the Ferromagnetically Coupled GdF_3. *J. Mater. Chem. C*, **2015**,**3**:12206-12211

[11]Chen Y C, Qin L, Meng Z S, Meng Z S, Yang D F, Wu C, Fu Z D, Zheng Y Z, Liu J L, Tarasenko R, Orendac M, Sechovsky V, Tong M L. Study of a Magnetic-Cooling Material $Gd(OH)CO_3$. *J. Mater. Chem. A*, **2014**,**2**:9851-9858

[12]Zhang Z M, Zangana K H, Kostopoulos A K, Tong M L, Winpenny R E P. A Pseudo-icosahedral Cage {Gd_{12}} Based on Aminomethylphosphonate. *Dalton Trans.*, **2016**,**45**:9041-9044

[13]Wang W M, He L Y, Wang X X, Shi Y, Wu Z L, Cui J Z. Linear-Shaped $Ln^{Ⅲ}_4$ and $Ln^{Ⅲ}_6$ Clusters Constructed by a Polydentate Schiff-Base Ligand and a β-Diketone Co-ligand: Structures, Fluorescence Properties, Magnetic Refrigeration and Single-Molecule Magnet Behavior. *Dalton Trans.*, **2019**,**48**:16744-16755

[14]Wang W M, Yue R X, Gao Y, Wang M J, Hao S S, Shi Y, Kang X M, Wu Z L. Large Magnetocaloric Effect and Remarkable Single-Molecule-Magnet Behavior in Triangle-Assembled $Ln^{Ⅲ}_6$ Clusters. *New J. Chem.*, **2019**,**43**:16639-16646

[15]Zheng X Y, Peng J B, Kong X J, Long L S, Zheng L S. Mixed-Anion Templated Cage-like Lanthanide Clusters: Gd_{27} and Dy_{27}. *Inorg. Chem. Front.*, **2016**,**3**:320-325

[16]Wang K, Chen Z L, Zou H H, Zhang S H, Li Y, Zhang X Q, Sun W Y, Liang F P. Diacylhydrazone Assembled {Ln_{11}} Nanoclusters Featuring a "Double-Boats Conformation" Topology: Synthesis, Structures and Magnetism. *Dalton Trans.*, **2018**,**47**:2337-2343

[17]Chen W P, Liao P Q, Jin P B, Zhang L, Ling B K, Wang S C, Chan Y T, Chen X M, Zheng Y Z. The Gigantic {NiGd} Hexagon: A Sulfate-Templated "Star-of-David" for Photocatalytic CO Reduction and Magnetic Cooling. *J. Am. Chem. Soc.*, **2020**,**142**:4663-4670

[18]Peng J B, Kong X J, Zhang Q C, Orendac M, Prokleska J, Ren Y P, Long L S, Zheng Z P, Zheng L S. Beauty, Symmetry, and Magnetocaloric Effect-Four-Shell Keplerates with 104 Lanthanide Atoms. *J. Am. Chem. Soc.*, **2014**,**136**:17938-17941

[19]Yin D D, Chen Q, Meng Y S, Sun H L, Zhang Y Q, Gao S. Slow Magnetic Relaxation in A Novel Carboxylate/Oxalate/Hydroxyl Bridged Dysprosium Layer. *Chem. Sci.*, **2015**,**6**:3095-3101

[20]Sun W B, Yan P F, Jiang S D, Wang B W, Zhang Y Q, Li H P, Chen P, Wang Z M, Gao S. High Symmetry or Low Symmetry, That is the Question-High Performance Dy(Ⅲ) Single-Ion Magnets by Electrostatic Potential Design. *Chem. Sci.*, **2016**,**7**:684-691

[21]Ishikawa N, Sugita M, Ishikawa T, Koshihara S Y, Kaizu Y. Lanthanide Double-Decker Complexes Functioning as Magnets at the Single-Molecular Level. *J. Am. Chem. Soc.*, **2003**,**125**:8694-8695

[22]Katagiri S, Tsukahara Y, Hasegawa Y, Wada Y. Energy-Transfer Mechanism in Photoluminescent Terbium (Ⅲ) Complexes Causing Their Temperature-Dependence. *Bull. Chem. Soc. Jpn.*, **2007**, **80**: 1492-1503

[23]Boudreaux E A, Mulay L N. *Theory and Applications of Molecular Paramagnetism*. New York: Wiley-Interscience, **1976**.

[24]Wang W M, Duan W W, Yue L C, Wang Y L, Ji W Y, Zhang C F, Fang M, Wu Z L. Magnetic Refrigeration and Single-Molecule Magnet Behaviour of Two Lanthanide Dinuclear Complexes (Ln=$Gd^{Ⅲ}$, $Tb^{Ⅲ}$) Based on 8-Hydroxyquinolin Derivatives. *Inorg. Chim. Acta*, **2017**, **466**:145-150

[25]Zhang H T, Ma L, Han M R, Feng S S, Zhu M L. A One-Dimensional Chiral Gadolinium Complex Based on a Tartaric Acid Derivative: Crystal Structure, Thermal Behavior and Magnetic Properties. *Inorg. Nano-Met. Chem.*, **2021**,**51**(6):761-765

[26]靳平宁, 闫瑞芳, 胡鹏, 吴燕妮, 高媛媛, 黄玲珠, 朱怡璇, 苏妍, 汪应灵. 基于席夫碱配体的Gd(Ⅲ)/Dy(Ⅲ)配合物的结构和磁性. 无机化学学报, **2018**,**34**(5):951-956
JIN P N, YAN R F, HU P, WU Y N, GAO Y Y, HUANG L Z, ZHU Y X, SU Y, WANG Y L. Dinuclear Gd(Ⅲ)/Dy(Ⅲ) Complexes Based on Schiff base Ligands: Structures and Magnetic Properties. *Chinese J. Inorg. Chem.*, **2018**,**34**(5):951-956

[27]Wang W M, Wang Q, Bai L, Qiao H, Zhao X Y, Xu M, Liu S Y, Shi Y, Fang M, Wu Z L. Lanthanide-Directed Fabrication of Fhree Phenoxo-O Bridged Dinuclear Complexes Showing Magnetic Refrigeration and Single-Molecule Magnet Behaviour. *Polyhedron*, **2018**, **142**:43-48

[28]Niu H J, Wang L H, Yang G E, Wang X X. Structures and Magnetic Refrigeration Properties of Three Gd_2 Complexes. *Inorg. Chim. Acta*, **2019**,**489**:155-159

[29]Han M R, Zhang H T, Wang J N, Feng S S, Lu L P. Three Chiral One-Dimensional Lanthanide-Ditoluoyl-Tartrate Bifunctional Polymers Exhibiting Luminescence and Magnetic Behaviors. *RSC Adv.*, **2019**, **9**:32288-32295

[30]Wang W M, Zhang H X, Wang S Y, Shen H Y, Gao H L, Cui J Z, Zhao B. Ligand Field Affected Single-Molecule Magnet Behavior of Lanthanide(Ⅲ) Dinuclear Complexes with an 8-Hydroxyquinoline Schiff Base Derivative as Bridging Ligand. *Inorg. Chem.*, **2015**,**54**: 10610-10622

[31]Yu Z P, Liu J, Feng X, Zhou K, Wang W M, Shi Y. Structures and Magnetic Properties of Two Series of Phenoxo-O Bridged Ln_2 Complexes: Two Gd_2 Complexes Displaying Magnetic Refrigeration Properties. *Inorg. Chim. Acta*, **2018**,**469**:105-110

[32]Xu C Y, Wu Z L, Fan C J, Yan L L, Wang W M, Ji B M. Synthesis of Two Lanthanide Clusters $Ln^{Ⅲ}_4$ (Gd_4 and Dy_4) with [2×2] Square Grid Shape: Magnetocaloric Effect and Slow Magnetic Relaxation Behaviors. *J. Rare Earths*, **2021**,**39**:1082-1088

[33]Wang K, Chen Z L, Zou H H, Hu K, Li H Y, Zhang Z, Sun W Y, Liang F P. A Single-Stranded $\{Gd_{18}\}$ Nanowheel with Symmetric Polydentate Diacylhydrazone Ligand. *Chem. Commun.*, **2016**, **52**: 8297-8300

[34]Wang W M, Xue C L, Jing R Y, Ma X, Yang L N, Luo S C, Wu Z L. Two Hexanuclear Lanthanide $Ln_6^{Ⅲ}$ Clusters Featuring Remarkable Magnetocaloric Effect and Slow Magnetic Relaxation Behavior. *New J. Chem.*, **2020**,**44**:18025-18030

[35]Cui C H, Ju W W, Luo X M, Lin Q F, Cao J P, Xu Y. A Series of Lanthanide Complexes Constructed from Ln_8 Rings Exhibiting Large Magnetocaloric Effect and Interesting Luminescence. *Inorg. Chem.*, **2018**,**57**:8608-8614

[36]Chang L X, Xiong G, Wang L, Cheng P, Zhao B. A 24-Gd Nanocapsule with a Large Magnetocaloric Effect. *Chem. Commun.*, **2013**,**49**: 1055-1057

[37]Guan X F, Shen J X, Hu X Y, Yang Y, Han X, Zhao J Q, Wang J, Shi Y, Wang W M. Synthesis, Structures and Magnetic Refrigeration Properties of Four Dinuclear Gadolinium Complexes. *Polyhedron*, **2019**,**166**:17-22

[38]Xia Q Y, Feng M Y, Ma D X, Shi S M, Xie Y C, Tian W, Shi H J, Wang Q L, Wang W M. Structures, Luminescent Properties and Magnetic Refrigeration of Two Series of $Ln^{Ⅲ}_2$ Complexes. *Polyhedron*, **2019**,**166**:141-145

[39]Wang S Y, Wang W M, Zhang H X, Shen H Y, Jiang L, Cui J Z, Gao H L. Seven Phenoxido-Bridged Complexes Encapsulated by 8-Hydroxyquinoline Schiff Base Derivatives and β-Diketone Ligands: Single-Molecule Magnet, Magnetic Refrigeration and Luminescence Properties. *Dalton Trans.*, **2016**,**45**:3362-3371

[40]Wang W M, Kang X M, Shen H Y, Wu Z L, Gao H L, Cui J Z. Modulating Single-Molecule Magnet Behavior Towards Multiple Magnetic Relaxation Processes through Structural Variation in Dy_4 Clusters. *Inorg. Chem. Front.*, **2018**,**5**:1876-1885

[41]Wang W M, Gao Y, Yue R X, Qiao N, Wang D T, Shi Y, Zhang H, Cui J Z. Construction of a Family of Ln_3 Clusters Using Multidentate Schiff Base and β-Diketonate Ligands: Fluorescent Properties, Magnetocaloric Effect and Slow Magnetic Relaxation. *New J. Chem.*, **2020**,**44**:9230-9237

[42]Han L J, Chen J, Zhang Z Q, Zhang H H, Kang T T, Wang W M, Mu S L, Shi Y. Synthesis, Structure and Slow Magnetic Relaxation of a Linear Ho_4 Cluster. *Inorg. Chem. Commun.*, **2018**,**96**:52-55

[43]Xu C Y, Qiao X Y, Tan Y, Liu S S, Hou W Y, Cui Y Y, Wu W L, Hua Y P, Wang W M. Modulating Single-Molecule Magnet Behaviors of $Dy^{Ⅲ}_4$ Clusters through Utilizing Two Different β-Diketonate Coligands. *Polyhedron*, **2019**,**160**:272-278

[44]Tian H Q, Huang F P, Li Y F, Chen P Q, Chai K Y, Lu J, Liu H T, Zeng S Y, Li D C, Dou J M. Ring-Forming Transformation Associated with Hydrazone Changes of Hexadecanuclear Dysprosium Phosphonates. *Dalton Trans.*, **2021**,**50**:1119-1125